Adaptive optics wide-field microscopy using direct wavefront sensing

Oscar Azucena,[1,*] Justin Crest,[2] Shaila Kotadia,[2] William Sullivan,[2] Xiaodong Tao,[1] Marc Reinig,[3] Donald Gavel,[3] Scot Olivier,[4] and Joel Kubby[1]

[1]*Jack Baskin School of Engineering, University of California, Santa Cruz, 1156 High Street, Santa Cruz, California 95064, USA*

[2]*Molecular, Cell, and Developmental Biology, University of California, Santa Cruz, 1156 High Street, Santa Cruz, California 95064, USA*

[3]*Laboratory for Adaptive Optics, University of California, Santa Cruz, 1156 High Street, Santa Cruz, California 95064, USA*

[4]*Physics and Advanced Technologies, Lawrence Livermore National Laboratory, 7000 East Avenue, Livermore, California 94550, USA*

**Corresponding author: azucena@soe.ucsc.edu*

Received November 22, 2010; revised January 31, 2011; accepted February 1, 2011; posted February 7, 2011 (Doc. ID 138521); published March 8, 2011

We report a technique for measuring and correcting the wavefront aberrations introduced by a biological sample using a Shack–Hartmann wavefront sensor, a fluorescent reference source, and a deformable mirror. The reference source and sample fluorescence are at different wavelengths to separate wavefront measurement and sample imaging. The measurement and correction at one wavelength improves the resolving power at a different wavelength, enabling the structure of the sample to be resolved. © 2011 Optical Society of America

OCIS codes: 220.1080, 160.2540, 010.7350.

Current methods for imaging biological samples suffer from degradation in the optical path brought upon by the sample itself [1–5]. The image degradation is caused by changes in the index of refraction along the optical path the light travels and thus is inherent, since many of the objects of interest require the sample to be in its original environment [1,2,6]. Adaptive optics (AO) is a technique for correcting images of objects by manipulating the wavefront of the incoming light [5,7]. AO is a technique used in astronomy to directly measure and correct the aberration introduced by turbulence in the optical path [7]. AO has also been applied to vision science to enhance our understanding of the human eye [8]. A typical AO system is composed of three main components: a wavefront sensor, a wavefront corrector (usually a deformable mirror), and a control system to communicate between the wavefront sensor and corrector. Most AO microscope systems so far have not directly measured the wavefront due to the complexity of adding a wavefront sensor in an optical system and the lack of point-source references [3] such as the "guide-stars" used in astronomy [7] and vision science [9,10]. Feierabend *et al.* developed a method of obtaining direct wavefront measurements in highly scattering samples by using a short pulse of light to accurately distinguish the light coming from focus [11]. This method worked well, but it requires a sample with a relatively high scattering coefficient.

A method for measuring the wavefront in biological samples is to inject a fluorescent bead into the specimen and use its fluorescent light as a reference source for a Shack–Hartmann wavefront sensor (SHWS) [12–14]. The injection of the fluorescent bead does not cause any significant damage to the live embryo since the needle used for injection is relative small (3–5 μm in diameter) and the embryo is able to repair the perforated membrane [12]. The peak emission of the reference source, a 1 μm diameter crimson bead at 647 nm (Invitrogen, Carlsbad, CA), is chosen to be different from the peak of the sample's green fluorescent emission at 510 nm (science object) [13] so that the two signals can be imaged separately. In addition to reducing the impact of photobleaching on the sample, the density of the guide stars can be chosen to be sparse, so that only one guide star will appear in the field of view of the SHWS. The advantage of this method is that it provides a pointlike source that is incoherent to the source of illumination, overcoming the disadvantages of using scattered light. This method also provides a direct way of measuring the wavefront as well as the effect of the corrections as the wavefront error can be constantly monitored in the AO system.

We present here the results of correcting the wavefront introduced by the tissue of a *Drosophila* embryo using a crimson fluorescent bead as a reference source. Verification of the method is provided by images of green fluorescent beads placed behind the embryo, showing the difference between the corrected image and the uncorrected image of the green beads. We demonstrate that this approach enables micrometer-scale features to be resolved through 20-μm-thick tissue that are not resolved without the use of adaptive optics. This provides a model system where we are able to emulate green fluorescent protein that is typically used in biology. The green fluorescent beads provide a science object with a well-defined structure and a size that can be known to subresolution accuracy.

Figure 1 shows the design of the adaptive optics wide-field microscope. An AO system was added to the back port of an Olympus IX71 inverted microscope (Olympus Microscope, Center Valley, PA). This allowed use of the side image port for point spread function (PSF) measurements that were compared to the PSF viewed after the AO system to ensure that the AO optical system did not add aberrations. Using a camera with very small pixels (flea2 with 4.65 μm pixels, Point Grey, NY), we were able to verify a very close match between the PSF before and after the AO system. The AO system was designed around an Olympus 60× oil immersion objective (Ob) with a numerical aperture of 1.42 and a working distance of 0.15 mm. Lenses L1 and L2 have 180 and 85 mm focal lengths, respectively, and are used to image the back pupil of the 60× objective onto the deformable mirror (DM) (Boston Micromachines, Boston, MA). The DM

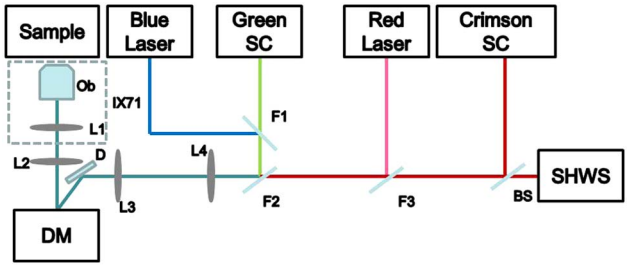

Fig. 1. (Color online) Adaptive optics wide-field microscope setup. L1, L2, L3, L4 are 180, 85, 275, and 225 mm focal length lenses, respectively. Fold mirror D helps to bring the optical path into alignment for the SHWS.

has 140 actuators on a square array with a pitch of 400 μm, a stroke of 3.5 μm, and a 4.4 mm aperture. Note that 0.5 μm of stroke was lost to AO path compensation and flattening of the deformable mirror. L3 and L4 are 275 and 225 mm focal length lenses, respectively, and are used to reimage the back pupil of the objective onto the SHWS. The system has two illumination and imaging arms; the first is a science arm in which we used a set of filters F1 and F2 (Semrock, Rochester, NY) to redirect a beam from an argon 488 nm laser (Blue Laser) to the objective for excitation of 1 μm green fluorescent beads (Invitrogen, Carlsbad, CA) that are placed behind the sample. The light emitted from the green fluorescent beads is imaged by the Green Science Camera (Green, SC). Filter F3 (Semrock) is used to redirect the HeNe 632.8 nm laser (Red Laser) through a confocal illuminator (not shown) onto the optical path for excitation of the crimson reference beads [12,14]. This confocal illuminator allows us to illuminate a single crimson reference bead to create a single diffraction limited spot. The beam splitter (BS) lets 90% of the emitted light coming from the crimson reference beads go to the SHWS for wavefront measurement and 10% for imaging in the Crimson Science Camera (Crimson, SC). The SHWS is composed of a 44 × 44 element lenslet array (AOA Inc., Cambridge, MA) and a cooled CCD camera (Roper Scientific, Acton, NJ).

The AO system starts by measuring the wavefront error using light coming from the crimson reference bead after passing through the embryo. All of the systematic errors are first removed by using a wavefront measured from a reference bead that is inside the same media as the biological sample [12,14]. That information is used to generate the DM voltages using a reconstruction matrix method [15]. Finally, the adaptive optics loop is closed by applying 10% of the current correction voltage to the DM until the wavefront error is minimized.

Wavefront measurements for the AO system were taken from light emitted by the crimson beads that had traveled through an Oregon-R wild type strain of *Drosophila Melanogaster* embryos and then into a SHWS [12–14]. The SHWS measurements showed that at 10 ms of integration the rms measurement error from each wavefront was less than 30 nm at a wavelength of 647 nm (i.e., less than 5% of a wavelength). The average peak-to-valley wavefront error introduced by the sample was approximately 765 nm, while the maximum was approximately 1290 nm. The average rms wavefront error was approximately 104 nm, though rms wavefront errors as high as 189 nm were found. The Zernike decomposition of the wavefront showed that spherical aberrations, like coma and astigmatism, were the dominant source. A general decrease in magnitude was also observed with an increase in Zernike values (i.e., low-order aberrations tend to dominate the wavefront error).

The importance of using an AO system with a SHWS is that we can use one source, in this case a crimson bead, to correct for the aberrations introduced by the tissue to make wavefront corrections for features at another wavelength of interest [12–14]. The images in Fig. 2 are of green fluorescent beads that were excited using the 488 nm laser and imaged with the green science camera. In Fig. 2(a) the adaptive optics system is off. We can see some detail about structures underneath the embryo, but we are not able to resolve the individual beads that make up the clumps of material shown in the image. In Fig. 2(b) the AO system had been turned on, and we can clearly resolve the individual 1 μm fluorescent beads. Figures 2(c) and 2(d) show cross-sectional profiles along the red lines in Figs. 2(a) and 2(b), respectively. These figures show that with the AO system on we can clearly resolve the individual beads, and thus are able to obtain higher resolution structural information. Even though the wavefront aberrations were measured using the crimson beads, the corrections applied to the mirror still improve the image of the green fluorescent beads, which are more than 100 nm apart in wavelength.

In conclusion, we have demonstrated the use of fluorescent beads as reference sources for a Shack–Hartmann wavefront sensor used in wavefront reconstruction. In particular, we have shown that a wavefront measurement and correction made at 647 nm increased the resolution

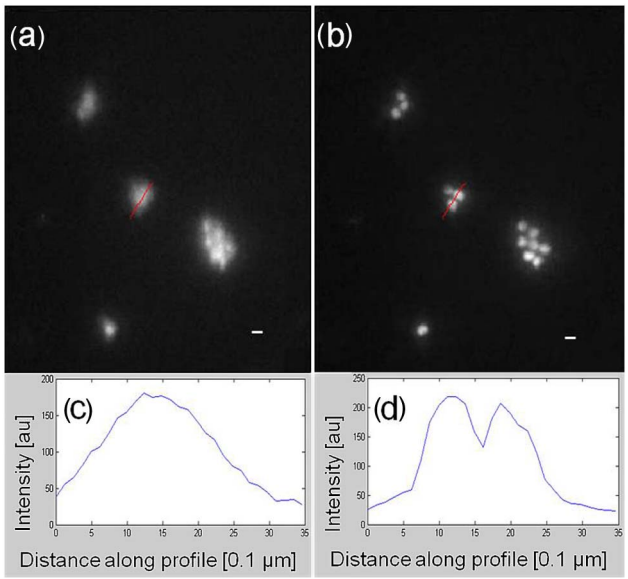

Fig. 2. (Color online) AO off and on. (a) Green science camera image with AO system off and (b) with AO on. (c) Profile display of red line in Fig. 2(a). (d) Profile display of red line in Fig. 2(b). (a) and (b) have been normalized to their own minimum and maximum to display the clear boundaries between the objects. The white lines in (a) and (b) are approximately 1 μm in length.

for an image gathered at 510 nm. This is due to the fact that the wavefront sensor measures the change in optical path difference, which does not vary significantly over a large portion of the visible spectrum.

This research was supported by a grant from the California Institute for Regenerative Medicine (grant RT1-01095-1). The contents of this publication are solely the responsibility of the authors and do not necessarily represent the official views of CIRM or any other agency of the State of California. This research was also supported by the National Institutes of Health (NIH) (grant NIH GM046409). We would like to thank Peter Kner at University of Georgia for useful conversations regarding this project.

References

1. T. Wilson, in *Confocal and Two-Photon Microscopy: Foundations, Applications, and Advances*, A. Diaspro, ed. (Wiley-Liss, 2002), p. 19.
2. K. Svoboda and R. Yasuda, Neuron **50**, 823 (2006).
3. M. J. Booth, Phil. Trans. R. Soc. A **365**, 2829 (2007).
4. A. Dunn and R. Richards-Kortum, IEEE J. Sel. Top. Quantum Electron. **2**, 898 (1996).
5. M. Schwertner, M. J. Booth, and T. Wilson, J. Microsc. **228**, 97 (2007).
6. J. B. Wyckoff, Y. Wang, E. Y. Lin, J. F. Li, S. Goswami, E. R. Stanley, J. E. Segall, J. W. Pollard, and J. Condeelis, Cancer Res. **67**, 2649 (2007).
7. J. W. Hardy, *Adaptive Optics for Astronomical Telescopes* (Oxford University Press, 1998).
8. J. Porter, H. Queener, J. Lin, K. Thorn, and A. Awwal, eds., *Adaptive Optics for Vision Science* (Wiley-Interscience, 2006).
9. J. Liang, B. Grim, S. Goelz, and J. F. Bille, J. Opt. Soc. Am. A **11**, 1949 (1994).
10. L. D. S. Haro and J. C. Dainty, Opt. Lett. **24**, 61 (1999).
11. M. Feierabend, M. Ruckel, and W. Denk, Opt. Lett. **29**, 2255 (2004).
12. O. Azucena, J. Crest, J. Cao, W. Sullivan, P. Kner, D. Gavel, D. Dillon, S. Olivier, and J. Kubby, Opt. Express **18**, 17521 (2010).
13. O. Azucena, J. Kubby, J. Crest, J. Cao, W. Sullivan, P. Kner, D. Gavel, D. Dillon, and S. Olivier, Proc. SPIE **7209**, 720906 (2009).
14. O. Azucena, J. Crest, J. Cao, W. Sullivan, P. Kner, D. Gavel, D. Dillon, S. Olivier, and J. Kubby, Proc. SPIE **7595**, 75950I (2010).
15. D. T. Gavel, Proc. SPIE **4839**, 972 (2003).